Article:
Lassila, T., Di Marco, L.Y., Mitolo, M. et al. (2017) Screening for Cognitive Impairment by Model Assisted Cerebral Blood Flow Estimation. IEEE Transactions on Biomedical Engineering. ISSN: 0018-9294

https://doi.org/10.1109/TBME.2017.2759511

Screening for Cognitive Impairment by Model Assisted Cerebral Blood Flow Estimation

Toni Lassila, Luigi Yuri Di Marco, Micaela Mitolo, Vincenzo Iaia, Giorgio Levedianos, Annalena Venneri, and Alejandro F. Frangi*, *Fellow, IEEE*

***Abstract*— *Objective:* Alzheimer's disease (AD) is a progressive and debilitating neurodegenerative disease; a major health concern in the ageing population with an estimated prevalence of 46 million dementia cases worldwide. Early diagnosis is therefore crucial so mitigating treatments can be initiated at an early stage. Cerebral hypoperfusion has been linked with blood-brain barrier dysfunction in the early stages of AD, and screening for chronic cerebral hypoperfusion in individuals has been proposed for improving the early diagnosis of AD. However, ambulatory measurements of cerebral blood flow are not routinely carried out in the clinical setting. In this study, we combine physiological modelling with Holter blood pressure monitoring and carotid ultrasound imaging to predict 24-hour cerebral blood flow (CBF) profiles in individuals. One hundred and three participants (53 with mild cognitive impairment (MCI), 50 healthy controls) underwent model-assisted prediction of 24-hour CBF. Model-predicted CBF and neuropsychological tests were features in lasso regression models for MCI diagnosis. *Results:* A CBF-enhanced classifier for diagnosing MCI performed better, area-under-the-curve (AUC) = 0.889 (95%-CI: 0.800 to 0.978), than a classifier based only on the neuropsychological test scores, AUC = 0.818 (95%-CI: 0.643 to 0.992). An additional cohort of 25 participants (11 MCI, 14 healthy) was recruited to perform model validation by arterial spin-labelling magnetic resonance imaging and to establish a link between measured CBF and that predicted by the model. *Conclusion:* Ultrasound imaging and ambulatory blood pressure measurements enhanced with physiological modelling can improve MCI diagnosis accuracy.**

Index Terms— Cerebral blood flow, biomedical monitoring, Alzheimer's disease, physiological modelling

I. Introduction

INCREASING evidence [1, 2, 3, 4, 5] links reduced cerebral blood flow (CBF) with development of sporadic Alzheimer's disease (AD). According to the vascular hypothesis of AD, a combination of natural ageing and vascular risk factors leads to chronic cerebral hypoperfusion that results in progressive blood-brain barrier dysfunction, increased oxidative stress and inflammation, and mitochondrial dysfunction. This disrupts neurovascular coupling and leads to the amyloid cascade and tau-pathologies that are hallmarks of AD [6].

Screening for cerebral hypoperfusion using a combination of carotid ultrasound, echocardiography, and ankle-brachial index monitoring has been proposed [7] to identify persons at-risk of developing AD. Both reduced CBF and elevated pulsatility index (PI) were associated with mild cognitive impairment (MCI) in meta-analysis of studies using transcranial Doppler ultrasonography or near-infrared spectroscopy to measure CBF [8]). If primary screening for such factors can be performed by non-invasive and affordable means, persons identified as at-risk could then be directed to a secondary screening consisting of neuropsychological tests, structural magnetic resonance imaging (sMRI), cerebrospinal fluid (CSF) sampling, regional cerebral blood flow (rCBF) imaging by single photon emission computer tomography (SPECT), or even positron emission tomography (PET) amyloid imaging.

Variability in CBF and blood pressure (BP) arises during the 24-hour circadian cycle due to effects of sleep, exercise, stress, and digestion. It would be desirable to perform ambulatory CBF monitoring rather than relying only on clinical spot examinations. There is evidence linking AD progression with decreased variability in CBF [8] and increased variability in BP [9]. Glucocorticoid hormone levels vary in 24-h cycles and dynamically increase with stress [10, 11]. Circadian rhythms of cortisol (a key glucocorticoid hormone) are associated with changes in heart rate [12, 13] and BP. Alteration of circadian rhythms has been associated with AD [14, 15] and circadian BP rhythms are altered in AD patients when compared with healthy controls [16]. Disruption of diurnal BP variation is closely associated with cognitive impairment [17]. However, many CBF imaging modalities are performed in a clinical setting and taking measurements during a person's normal daily activities are impossible.

We propose a data-driven model for predicting 24-hour variability of CBF based on combined ambulatory measurements and physiological modelling of the circulatory system and cerebral autoregulation. A lumped-parameter circulation model is driven by ambulatory blood pressure and heart rate measurements and used to predict 24-hour total CBF (tCBF) profiles in individuals. The model predicted tCBF is compared against both clinical ultrasound spot measurements and magnetic resonance perfusion imaging to establish model validity. We then explore how model-predicted tCBF can be used in conjunction with standard

Manuscript received June 19, 2017; accepted October 1, 2017. Work supported by a grant from the European Research Council Seventh Framework Programme [FP7-ICT-2011-5.2-601055 VPH-DARE@IT]. We acknowledge the data processing of M. Lange and A. Sarrami-Foroushani.
T. Lassila and A.F. Frangi (correspondence: a.frangi@sheffield.ac.uk) are with the CISTIB, University of Sheffield, UK. L.Y. Di Marco was previously with the same institute.

V. Iaia, and G. Levedianos are with the IRCCS Fondazione Ospedale San Camillo, Lido di Venezia, Italy. M. Mitolo was previously at the same institute and is currently with the Functional MR Unit, Policlinico S.Orsola e Malpighi, Department of Biomedical and NeuroMotor Sciences (DiBiNeM), Bologna. A. Venneri is with the Department of Neuroscience, University of Sheffield, UK.

neuropsychological tests to aid in the classification of MCI, often a prodromal stage of AD. By training lasso regression models for the binary classification problem of discriminating MCIs from cognitively healthy controls, we demonstrate that adding model-predicted tCBF values can improve classification accuracy. The accuracy of the diagnostic test is compared to machine learning approaches utilising structural MRI biomarkers from the literature (reviewed in [18, 19]).

II. Subjects and Methods

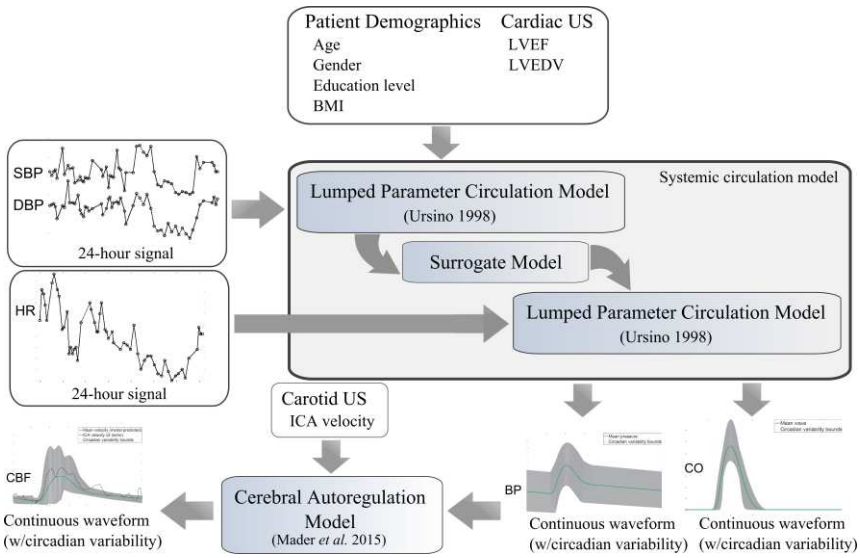

Fig. 1. Person-specific modelling pipeline for predicting circadian variability in cerebral perfusion waveforms. Components with white background represent person-specific measurements, components with shaded background represent mathematical models.

A. Clinical and ambulatory data collection

The data were collected at the Istituto di Ricovero e Cura a Carattere Scientifico (IRCCS) Fondazione Ospedale San Camillo, Venezia Lido, Italy, and included 103 people (50 cognitively healthy controls, age 71 ± 8 years, and 53 with MCI, age 75 ± 7 years). Exclusion criteria included diagnostic entities of clinical concern, chronic or acute cerebrovascular disease as main aetiology, history of transient ischemic attacks, presence of uncontrolled brain seizures, peptic ulcer, cardiovascular disease, sick-sinus syndrome, neuropathy with conduction difficulties, proof of abnormal levels of folates, vitamin B12 or thyroid-stimulating hormone, significant neuropsychiatric symptoms, treatment with medication for research purposes or with toxic effects to internal organs. Participants with significant disabilities, or with sMRI indication of a major diagnostic category of non-neurodegenerative nature, which could otherwise explain cognitive symptoms, were not considered for recruitment. The joint ethics committee of the Health Authority Venice 12 and the IRCCS Fondazione Ospedale San Camillo (Protocol number 2014.08) approved the study and all participants gave informed consent prior to participation in the study.

Each participant underwent examinations during five days. For 24-hours, the participants wore a Holter device (Cardioline walk200b, Cardioline S.p.A., Milan, Italy) that recorded systolic and diastolic blood pressure and heart rate (SBP/DBP/HR) every 15 minutes during daytime and every 30 minutes at night. The participants were imaged with carotid ultrasound (Siemens Acuson X300PE, Siemens Healthineers, Erlangen, Germany) and cardiac ultrasound (Siemens Acuson SC2000, Siemens Healthineers, Erlangen, Germany) to estimate internal carotid artery (ICA) flow velocities and cardiac left ventricle volumetric indices (ejection fraction and end-diastolic volume). The ICA velocity measurements were recorded for both left and right internal carotids and digitised from the images. Underestimation bias in the left ventricular end-diastolic volume and ejection fraction were corrected for, following [20]. Echocardiographic estimation of chamber volumes failed in 24 cases – for these participants the values were estimated by *k*-nearest neighbour imputation with *k*=10.

Each participant was assessed with a battery of neuropsychological tests. These included the Stroop test, Mini Mental State Examination (MMSE), Rey complex figure test, Token test, Phonemic/Semantic fluency tests, Raven's coloured progressive matrices (RCPM), Digit Cancellation test, Paired Associates Learning test, Spatial supra-span test, and the Corsi test. Test scores were corrected for age, education and gender as necessary. Ground-truth diagnosis of MCI status was obtained according to Petersen's criteria [21]. Diagnostic status was reached by multidisciplinary consensus based on clinical, neuropsychological and neuroimaging evidence and clinical follow ups at regular intervals.

B. Personalised lumped-parameter circulation model

While the carotid ultrasound examination provides a view of instantaneous blood flow into the brain, it cannot measure the circadian variability of CBF without disrupting the participant's normal daily activities. We therefore constructed a computational model that took the 24-hour SBP/DBP/HR measurements as input data, and generated continuous waveforms of BP, cardiac output (CO), and CBF as outputs.

A lumped parameter circulation model (LPCM) [22] was used to simulate circulatory flow and to predict systemic BP and cardiac output (CO). The model contained a four-chamber model of the heart, plus a compartmental model of the systemic arteries/veins, pulmonary arteries/veins, and splanchnic arteries/veins. The LPCM had 26 equations and 84 model parameters, which are provided in the Supplementary Material. Reference parameter values in [22]

are given for young and healthy adults only. Model personalisation was therefore needed.

We targeted five model parameters for personalisation, following a literature review of age, gender, and lifestyle-related changes in the circulatory system [23, 24, 25, 26]. They were: (i) total blood volume (V_{tot}), (ii) systemic arterial compliance (C_{sa}), (iii) systemic arterial resistance (R_{sa}), (iv) systolic interval length (L_{si}), and (v) cardiac chamber volume (V_{cc}). These parameters were optimised around the reference values given in [22] within the 80% to 120% range for V_{tot} and 60% to 140% range for the other variables. Five simulation outputs were matched with 24-hour ambulatory measurements: diastolic blood pressure (DBP) P_D, systolic blood pressure (SBP) P_S, LV ejection fraction E_f, and LV end-diastolic volume $V_{\mathrm{lv,ed}}$. The LPCM was run until a periodic steady state was reached (~50 s of simulation time), and CBF values were recorded from the last heartbeat.

C. Surrogate modelling of the LPCM

To accelerate the personalisation of the LPCM model, we constructed a surrogate model to approximate its input-output response. This surrogate model used as predictors the five model parameters

$$x = (V_{\mathrm{tot}}, C_{\mathrm{sa}}, R_{\mathrm{sa}}, L_{\mathrm{si}}, V_{\mathrm{cc}}) \tag{1}$$

as linear and quadratic factors, and explained the observed dependent variables $y = (P_D, P_S, E_f, V_{\mathrm{lv,ed}})$ using the surrogate model:

$$y_i(x) = \sum_{j=1}^{5}\left(\alpha_{i,j}x_j + \beta_{i,j}x_j^2\right) \tag{2}$$

for i=1,…,5. The response surfaces for each of the dependent variables were built by sampling the model parameter space using a central composite design with 27 output evaluations (the centre point was included 9 times to reduce bias), followed by multivariate regression to identify the coefficients $\alpha_{i,j}$ and $\beta_{i,j}$.

D. Calibration of model parameters from Holter BP

Once the surrogate model was generated, it was used to infer the values of the model parameters through a nonlinear fitting procedure. The Holter-measured HR values were used directly as inputs by running the LPCM in an open-loop configuration. In this configuration, the vagal parasympathetic regulation was disabled in the LPCM model and the value of HR was directly prescribed. For each time point t^k during the 24-hour period, we took the values of $y_1^k = P_D(t_k)$, $y_2^k = P_S(t_k)$, $y_3^k = E_f$, $y_4^k = V_{\mathrm{lv,ed}}$, and solved a nonlinear multi-objective optimisation problem to find the vector x^k so

$$\min_{x^k}\left\{\sum_{j=1}^{4}\left|\frac{y_j^k - \widetilde{y_j^k}(x^k)}{y_j^*}\right| + \nu\sum_{i=1}^{5}\left|x_i^k - 1\right|^2\right\}, \tag{3}$$

where the reference values $P_D^* = 60$ mmHg, $P_S^* = 120$ mmHg, $E_f^* = 50\%$, and $V_{\mathrm{lv,ed}}^* = 120$ ml were used to scale the quantities, and the values $w_1 = w_2 = 10$ and $w_3 = w_4 = 1$ were used to weight fitting the SBP/DBP values over the other two quantities. A penalisation weight $\nu = 1$ was used to avoid parameter overfitting.

Once the optimal LPCM parameter vector x^k for each measurement time point t^k during the 24-hour period was found using the surrogate model, the same parameter values were used to run the full-order LPCM until a periodic steady state was reached, after which the waveforms for BP and CO were then extracted from the last heartbeat.

E. Model prediction of 24-h variability of CBF

The outputs of the LPCM acted as inputs to a *cerebral autoregulation model* (CAM) proposed in [27] that predicted cerebral artery flow. The CAM is based on a two-component viscoelastic model and was used in this work to derive middle cerebral artery (MCA) flow velocity waveforms during the 24-hour period.

The baseline (end-diastolic) flow velocity v_{bas} was a parameter to be defined in the CAM. Clinical ultrasound measurements of ICA flow velocity were used to define the baseline flow. These were translated into MCA flow velocities (the controlled quantity in the CAM). Experimental evidence suggests that the MCA flow velocity has a linear relationship to the ICA flow velocity, where the proportionality constant increases significantly with age in women but not in men [28]. This justified writing the MCA flow velocity as a function of the ICA flow velocity $v_{\mathrm{MCA}} = \gamma v_{\mathrm{ICA}}$, where γ=2.00 for men and γ=1.67+0.005×AGE for women. The CAM was run for 10 heartbeats using as input each BP waveform extracted from the LPCM. Finally, the MCA flow velocity waveform was extracted from the last heartbeat. With the previously described outputs from the LPCM, the output of the joint model comprised CO, BP, and CBF waveforms for each of the measurement periods during the 24-hour period. Volumetric ICA flow rates were estimated using the ultrasound-measured ICA diameters, followed by summing the flow contributions from left and right carotids. Systolic BP and arterial pulse pressure (APP) were measured from the model output BP. The pulsatility index (PI) was measured from the model-predicted MCA blood flow velocity. Both 24-hour mean values and coefficients of variability were recorded for each of the five CBF-related model outputs. The pipeline is shown in Fig. 1.

F. Lasso regression-based classifiers for MCI

To test the utility of model-derived CBF values in the diagnosis of MCI, we trained lasso regression models (LRM) for binary classification between MCI patients and cognitively normal controls with simultaneous feature selection and learning. Three models were trained to classify MCI:

(i) In Model A only demographic variables (gender, age, education, body mass index) and neuropsychological test scores (MMSE, Stroop test, Rey complex figure, RCPM, Phonemic/Semantic fluency, Token test, Digit Cancellation Test, Paired Associates Learning Test, Spatial supra-span, Corsi test) were used to train a LRM:

$$\min_{\beta_0,\beta_D,\beta_C}\left\{\frac{1}{2N}\sum_{n=1}^{N}\left(Y_n - \beta_0 - X_{n,D}\beta_D - X_{n,C}\beta_C\right)^2\right\} \tag{5}$$

subject to the lasso constraint

$$\sum_{i_D}\left|\beta_D^{i_D}\right| + \sum_{i_C}\left|\beta_C^{i_C}\right| \le \lambda, \tag{6}$$

where Y_n was a binary vector containing the MCI status of each participant in the training set, $X_{n,D}$ and $X_{n,C}$ denote the

demographic variables and neuropsychological test scores of the *n*th participant in the training set, respectively, β_0 was the model intercept, β_D and β_C were the regression weights for demographic and neuropsychological variables, respectively, and λ was a model hyperparameter to be tuned. Finally, a participant $(\widetilde{X_D}, \widetilde{X_C})$ not included in the training set was diagnosed as MCI by the model if

$$\beta_0 + \widetilde{X_D}\beta_D + \widetilde{X_C}\beta_C \geq Y_{\text{cut-off}}, \tag{7}$$

for some $Y_{\text{cut-off}} \in (0,1)$ to be chosen optimally. This model was taken as a baseline model for MCI diagnosis.

(ii) In Model B the demographic variables together with CBF variables were used to train the LRM

$$\min_{\beta_0,\beta_D,\beta_F} \left\{\frac{1}{2N}\sum_{n=1}^{N}\left(Y_n - \beta_0 - X_{n,D}\beta_D - X_{n,F}\beta_F\right)^2\right\} \tag{8}$$

subject to the lasso constraint

$$\sum_{i_D}\left|\beta_D^{i_D}\right| + \sum_{i_F}\left|\beta_F^{i_F}\right| \leq \lambda. \tag{9}$$

The same cut-off $Y_{\text{cut-off}}$ and decision rule (7) as in Model A were used to threshold Y_n and make a binary prediction.

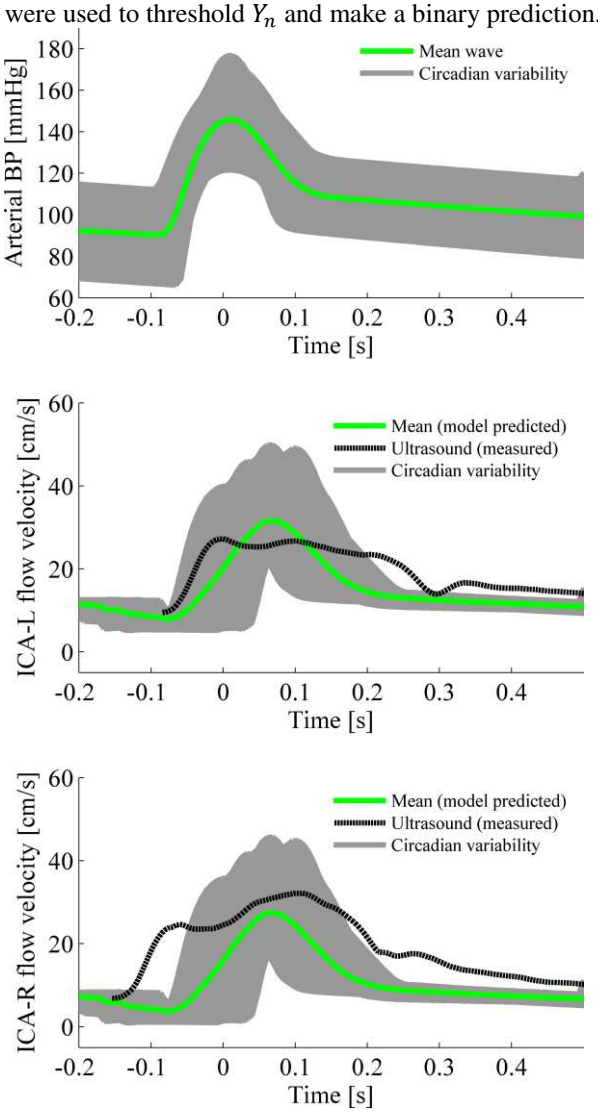

Fig. 2. Model predicted mean waveforms and circadian variability for CO (first row), systemic BP (second row), and flow velocity (third and fourth row) with one 61 y.o. MCI patient. Ultrasound measured ICA flow velocity signal superimposed on the model-predicted CBF plot. Systolic peak at t=0.

(iii) In Model C both neuropsychological test scores and CBF predictions were combined. We did not perform feature selection on the combined set of features, as neuropsychological test scores are discrete while CBF measurements are continuous, which may lead to suboptimal models [29]. Instead, Models A and B were combined using an OR-rule, i.e. a diagnosis of MCI was made if at least one test was positive. The rationale for this was that a combination of two diagnostic tests with high specificity but lower sensitivity (typical for AD classifiers) may provide more sensitive diagnostics.

In all three models, 4-fold cross-validation was performed to evaluate model performance. For Models A and B, the hyperparameter λ was optimised within the range $\lambda \in [10^{-4}, 10^{-1}]$ by using as optimisation criteria the area under the curve (AUC) of the receiver-operating characteristic (ROC) -curve obtained by varying $Y_{\text{cut-off}}$. The resulting optimal hyperparameters for models A and B were then used as-is in Model C to generate a combined model.

G. Comparison of tCBF and ASL-MRI derived rCBF

For validation of model-predicted tCBF against perfusion imaging of rCBF by arterial spin labelling MRI (ASL-MRI), a validation cohort of *N*=25 study participants (15 cognitively healthy controls, age 74 ± 5 years, and 10 with diagnosed MCI, age 75 ± 8 years) was recruited at the same centre. These additional participants were imaged using pseudo-continuous arterial spin labelling (pCASL) (Ingenia 3.0T CX, Philips Healthcare) using these parameters: sequence repetition time/echo time (TR/TE), 4,000 ms/14 ms; flip angle, 40°; field of view, 240 mm x 240 mm; matrix size, 80x80; 17 slices; thickness, 7 mm; labelling duration, 1.65 s; post-labelling delay, 1.525 s; and labelling gap, 20 mm.

SPM12 was used for the registration of the ASL-MRI perfusion maps against T1-weighted structural images. They were consequently equipped with maximum probability tissue labels defined on the MNI152 atlas, provided by Neuromorphometrics, Inc. (http://neuromorphometrics.com/) from data collected in the OASIS project (http://www.oasis-brains.org/). These labels were then used to estimate mean rCBF within each labelled region. We used the tissue probability map to also estimate the volumes of white and grey matter. The total model-predicted ICA flow (L+R) was then divided by the WM+GM volumes to obtain an estimate of total perfusion. An age-correction by linear regression was applied to the rCBF values. The age-corrected rCBF values were converted to *z*-scores by normalising them with the whole-cohort variance of rCBF within each region of interest (RoI). These were cortical regions reported to experience hypoperfusion in early stages of AD and MCI. Hypoperfusion in AD patients has been identified in the hippocampus, posterior cingulate, and the precuneus [30] (*N*=327), and in the superior parietal lobule of AD and amnestic MCI patients [31] (*N*=53). The rCBF in each RoI was then compared to the total perfusion in each participant.

III. RESULTS

A. Model predictions of tCBF in a MCI patient

Temporal wave forms of cardiac output, SBP, and ICA flow velocity produced by the LPCM are shown in Fig. 2 for one middle-aged (61 y.o.), female participant with MCI. The ICA velocity waveform (from ultrasound) is superimposed on the 24-hour variability envelope (in grey). During the 24-hour

data collection period, 74 BP measurements were made by the Holter device, of which eight were deemed failed by the Holter system and discarded. The remaining observations were used to calibrate the patient-specific LPCM models and to simulate CBF profiles at 66 instances in time. A summary of the model-predicted 24-hour CBF profile compared with clinical ultrasound measurements is given in Table 1. The measured ICA flow velocity matched closely the mean of the model-predictions. The model overestimated PI values, although the ICA-R PI value fell within the 95% confidence interval of the 24-hour variability bounds predicted by the model. Model predicted APP variability was compared against the Holter recording of APP variability, which was slightly overestimated by the model.

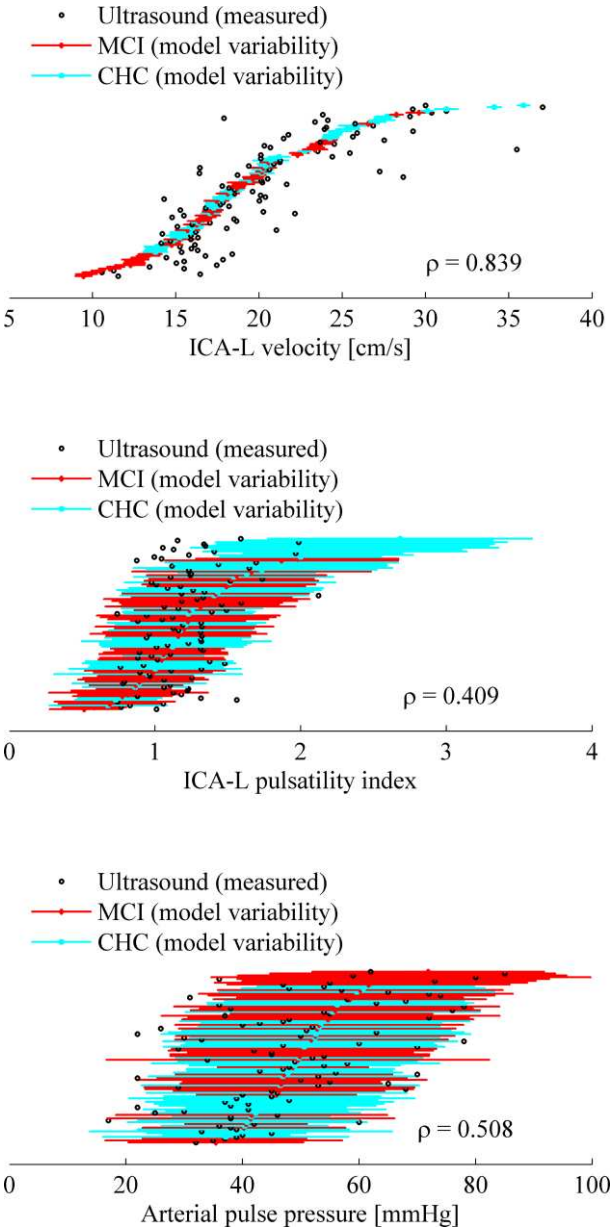

Fig. 3. Correlation plots between ultrasound measured (∘) and model predicted (◇ for MCI, ⊡ for CHC) flow rate in ICA-L (first row), pulsatility index in ICA-L (second row), and arterial pulse pressure (third row). Plots for ICA-R are similar and correlation coefficients are reported in the text.

TABLE 1
MODEL PREDICTED 24-HOUR CBF VS. ULTRASOUND-MEASURED CBF

CBF characteristic values	24-h model predicted	Measurement
ICA-L velocity (cm/s)	15.3 (0.5)	15.9
ICA-R velocity (cm/s)	15.1 (0.5)	16.1
ICA-L pulsatility index	2.02 (0.38)	1.12
ICA-R pulsatility index	2.04 (0.38)	1.57
Arterial pulse pressure (mmHg)	61.4 (11.7)	54.8 (14.2)

Model-predicted versus measured CBF values in the ICA for one 61 y.o. female MCI patient. Model-predicted values denote 24-h means and standard deviations (in parenthesis).

B. Comparison of modelled CBF and carotid ultrasound

We compared the model predicted CBF against ultrasound flow rate measurements at the carotid bifurcations for N=95 cases for validation. Waveform extraction failed in N=8 cases. For comparison, the model-predicted MCA flow velocities were converted into ICA flow velocities using the formula from [28]. The correlation plots in Fig. 3 show the model predicted 24-hour variability bounds for ICA-L flow velocity, ICA-L PI, and APP for both MCIs (◇) and cognitively healthy controls (CHC, ⊡) compared to the clinical ultrasound measurements (∘). As the CAM maintained the mean flow nearly constant, the 24-hour variability of CBF predicted by the model was small. While some outliers existed, good correlation was obtained between measured and model-predicted CBF (Pearson's ϱ=0.839 for ICA-L and ϱ=0.832 for ICA-R). The model-predicted variability of the PI was much larger and the correlation with ultrasound measurements was considerably weaker (Pearson's ϱ=0.409 for ICA-L and ϱ=0.381 for ICA-R). Usually the measured PI fell on the lower end of the variability bounds, indicating that the model overestimated PI. The model predicted APP also displayed large variability within the 24-hour period, but the correlation to measured APP was moderate (Pearson's ϱ=0.508) and the measured PI fell within the variability bounds.

C. Classification of MCI vs. healthy controls

Model-predicted CBF was characterised by four covariates with predictive value in the early diagnosis of dementia: ICA flow rate (total L+R), SBP, APP, and ICA PI (average of L and R). Means and coefficients of variation were computed for each CBF-derived quantity. Summary statistics of all these covariates are reported in Table 2 with the neuropsychological test scores and demographics variables. In univariate analysis, statistically significant differences between cognitively healthy controls (CHCs) and MCIs at the p<0.05 significance level were found to exist in these variables: age, education level, total ICA flow (24-h mean), APP (24-h mean), PI (24-h mean), besides several of the neuropsychological test scores.

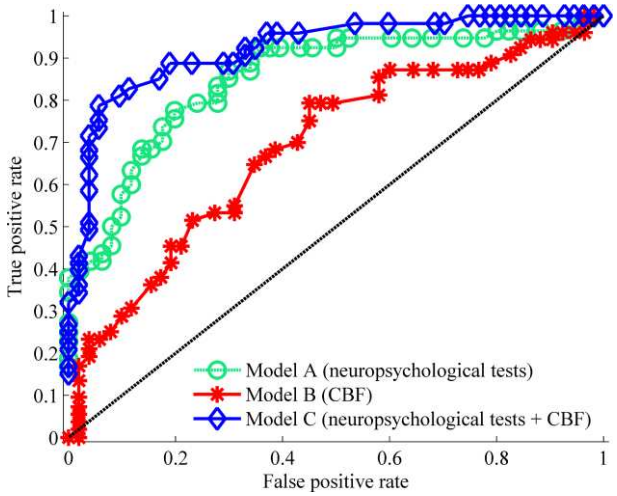

Fig. 4. ROC-curve for logistic regression classifiers for MCI trained using three covariate sets: MMSE and demographics only, CBF and demographics only, and CBF + MMSE and demographics.

The optimal value of the hyperparameter λ in the lasso-model was λ=0.04 for both Models A and B. The selected features are shown in the rightmost column of Table 2, where each asterisk denotes one fold of cross-validation where this feature was selected, so that **** denotes features selected in each of the four folds, etc. The receiver-operating characteristic -curves for all three models are shown in Fig. 4. Model A achieved an AUC = 0.818 (95%-CI: 0.643 to 0.992), Model B achieved an AUC = 0.698 (95%-CI: 0.444 to 0.952), and Model C achieved an AUC = 0.889 (95%-CI: 0.800 to 0.978). Optimal cut-off points were found by maximising balanced accuracy, resulting in a balanced accuracy of 87%, sensitivity of 81%, and specificity of 94% for Model C. The optimal cut-off values for each of the three models were $Y^{A}_{\mathrm{cut-off}} = 0.34$, $Y^{B}_{\mathrm{cut-off}} = 0.64$, and $Y^{C}_{\mathrm{cut-off}} = 0.64$.

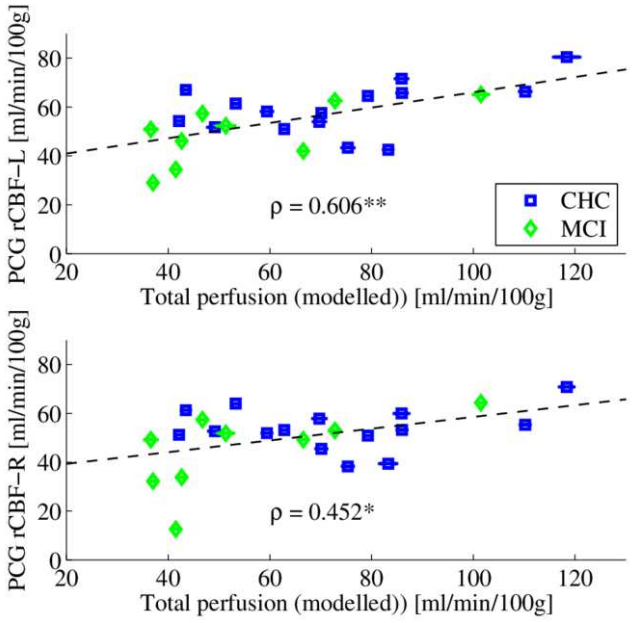

Fig. 5 Correlation plot between model-predicted tCBF and ASL-MRI measured rCBF in the left hippocampus (top) and right hippocampus (bottom), quantified by MCI status (◇ for MCI, ⊡ for CHC). Significance with p<0.05 indicated by * and significance with p<0.01 indicated by **.

D. Comparison of tCBF and ASL-MRI derived rCBF

Statistics of rCBF by cortical region measured in the validation cohort by ASL-MRI are given in Table 3. The acquisition in one MCI patient was identified by visual inspection to have failed in the left hemisphere with no corresponding defects visible in structural images. This participant was excluded from further analysis, leaving *N*=24 cases. Cerebral white matter, the hippocampus, superior parietal lobules, posterior cingulate gyrii, and the precuneus all had bilaterally lower CBF in the MCI patient, although only some differences were significant at p<0.05 due to the large between-subject variance of ASL-MRI measurements. Correlation between rCBF and total perfusion was measured in *N*=22 cases to evaluate the relationship between ambulatory tCBF estimates and clinical perfusion imaging. In two MCI patients, tCBF could not be estimated due to noisy ultrasound measurements. These cases were excluded from the correlation analysis. Correlation was low to moderate in the controls, but moderate to high in MCI patients. The correlation between rCBF in the hippocampus and 24-hour total perfusion as predicted by the model is shown in Fig. 5. Two MCI cases and one control exhibited bilateral hypoperfusion (<45 ml/min/100g), and two additional MCI cases exhibited unilateral hypoperfusion. The difficulty in obtaining significant correlations is due to the rCBF measurements being fluctuating quantities that depend on the level of brain activity, while tCBF is a 24-h mean point estimate. The rCBF signal is only partially explained by the total ICA flow into the brain. These associations will be weaker in the sub-cortical regions supplied by collateral circulation from the vertebral arteries (not estimated in this study). Regardless, the resulting correlations are positive and the MCI cases with significant hypoperfusion can be identified from both the ASL-MRI measured rCBF and the model-predicted total perfusion.

To validate the MCI classifier, Models A, B, and C were applied directly in the validation cohort using the model hyperparameters and optimal cut-offs in the original cohort. Model A resulted applied in the validation cohort resulted in a balanced accuracy of 67%, sensitivity of 88%, and specificity of 42%, whereas Model C resulted in a balanced accuracy of 80%, sensitivity of 88%, and specificity of 75%.

IV. Conclusions

Public health policy recommendations [32, 33] do not support population-wide screening for Alzheimer's disease. These recommendations are based on neuropsychological tests, with low positive predictive value in individuals under the age of 80. There is, however, a possibility that incorporating proxy measurements related to vascular risk factors in the screening program may improve early detection of MCI, since hypoperfusion occurs in some AD patients even before neurodegeneration with cognitive impairment occurs.

TABLE 2
NEUROPSYCHOLOGICAL TEST SCORES AND CBF IN THE TRAINING COHORT

	CHC (*N*=50)	MCI (*N*=53)	*p*	A	B
Men/Women	24 / 26	17 / 36	0.010*	****	**
Age	71.7 (7.9)	75.1 (6.7)	0.020*	***	***
Education (years)	12.8 (5.9)	9.6 (4.2)	0.001**	****	****
Body mass index	26.0 (3.1)	25.2 (4.1)	<0.001**		****
Mini Mental State Exam	27.5 (1.9)	24.6 (3.4)	<0.001**	**	
Stroop error interference	0.23 (0.89)	5.35 (7.71)	<0.001**	****	
Digit span forward	6.09 (0.93)	5.46 (0.93)	0.001**	**	
Stroop time interference	15.2 (9.0)	30.4 (30.9)	0.001**		
RCPM	33.7 (10.8)	30.0 (12.4)	0.108	*	
Phonemic fluency	30.2 (3.4)	25.9 (5.7)	<0.001**		

Semantic fluency	41.4 (6.8)	32.1 (11.8)	<0.001**	**	
Digit cancellation	51.8 (7.4)	45.3 (10.1)	<0.001**	*	
Token test	33.8 (2.2)	31.2 (3.0)	<0.001**	****	
Paired Associates Learning	12.1 (3.9)	9.0 (3.9)	<0.001**	**	
Spatial supra-span	20.1 (7.1)	13.5 (8.2)	<0.001**	***	
Corsi test	5.80 (5.8)	4.70 (1.1)	0.172	**	
Rey complex figure copy	34.7 (2.1)	26.8 (8.9)	<0.001**	****	
Rey complex figure recall	18.0 (5.3)	11.0 (5.3)	<0.001**	****	
Total ICA flow (24-h mean)	912 (271)	737 (237)	0.001**		****
SBP (mean)	128 (8)	132 (13)	0.084		
APP (24-h mean)	48.3 (6.2)	52.5 (9.8)	0.012*		
Pulsatility index (24-h mean)	1.19 (0.31)	1.48 (0.55)	0.002**		****
Total ICA flow (24-h CoV %)	1.51 (0.64)	1.82 (0.73)	0.023*		*
SBP (24-h CoV %)	10.8 (1.9)	11.0 (2.6)	0.633		**
APP (24-h CoV %)	21.8 (3.6)	21.9 (4.5)	0.948		*
Pulsatility index (24-h CoV %)	22.0 (3.6)	21.8 (4.6)	0.805		

Classification features in the training cohort, group-wise means and standard deviations (in parenthesis) between the two groups (CHC = cognitively healthy control, MCI = mild cognitive impairment), and their statistical significance in univariate analysis (two-sample *t*-test used for binary variates, one-way ANOVA test used for continuous variates). Frequency of feature selection in four-way cross-validation indicated by the number of asterisks in the two right-most columns.

TABLE 3
REGIONAL CBF IN THE VALIDATION COHORT

Demographics	CHC (*N*=15)	MCI (*N*=9)	*p*
Men/Women	4 / 11	3 / 6	0.742
Age	73.7 (5.1)	74.8 (7.8)	0.674
Education (years)	11.9 (2.9)	9.2 (3.4)	0.055
BMI	25.3 (3.3)	26.8 (3.6)	0.303
Total CBF (model predicted)			
Total ICA flow (R) [ml/min]	372 (174)	295 (170)	0.299
Total ICA flow (L) [ml/min]	388 (111)	278 (98)	0.022*
Perfusion [ml/min/100g]	72.6 (22.4)	55.2 (21.5)	0.075
Regional CBF (ASL-MRI) [z-score]			
Cerebral WM (R)	0.32 (0.88)	-0.42 (0.81)	0.053
Cerebral WM (L)	0.35 (0.79)	-0.30 (0.64)	0.048*
Cerebellar WM (R)	0.22 (0.91)	-0.36 (0.66)	0.107
Cerebellar WM (L)	0.21 (0.91)	-0.29 (0.70)	0.171
Hippocampus (R)	0.32 (0.69)	-0.38 (1.25)	0.090
Hippocampus (L)	0.40 (0.77)	-0.42 (0.96)	0.032*
Superior parietal lobule (R)	0.24 (1.10)	-0.48 (0.80)	0.102
Superior parietal lobule (L)	0.31 (1.01)	-0.31 (0.66)	0.116
Posterior cingulate gyrus (R)	0.31 (1.00)	-0.35 (0.67)	0.096
Posterior cingulate gyrus (L)	0.40 (0.97)	-0.43 (0.47)	0.026*
Precuneus (R)	0.26 (1.02)	-0.40 (0.50)	0.084
Precuneus (L)	0.32 (0.97)	-0.42 (0.44)	0.042*
Correlation coefficient between total perfusion and rCBF			
Cerebral WM (R)	0.22	0.39	
Cerebral WM (L)	0.27	0.36	
Cerebellar WM (R)	0.24	0.35	
Cerebellar WM (L)	0.15	0.72*	0.030
Hippocampus (R)	0.16	0.62	
Hippocampus (L)	0.45	0.66	
Superior parietal lobule (R)	0.20	0.52	
Superior parietal lobule (L)	0.21	0.40	
Posterior cingulate gyrus (R)	0.20	0.43	
Posterior cingulate gyrus (L)	0.23	0.33	
Precuneus (R)	0.22	0.83**	0.006
Precuneus (L)	0.29	0.73*	0.026

Between-groups rCBF differences in the validation cohort (CHC = cognitively healthy control, MCI = mild cognitive impairment), group-wise means and standard deviations (in parenthesis), and their statistical significance in univariate analysis (two-sample *t*-test used for binary variates, one-way ANOVA test used for continuous variates). Pearson correlation reported between rCBF (measured by ASL-MRI) and tCBF (model-predicted 24-hour mean). Significance with $p<0.05$ denoted by *, $p<0.01$ denoted by **.

In this study, ambulatory BP measurements and model-enhanced predictions were combined to predict individualised 24-hour CBF profiles. These were then combined with neuropsychological test scores to perform lasso regression, which was used for simultaneous feature selection and classification of MCI vs. CHC. We developed three models for detecting MCI. In a classifier based on neuropsychological test scores, 12 neuropsychological test scores were chosen by the algorithm as classification features. In the second model, six CBF-related quantities were chosen as classification features, but only the total ICA flow rate (24-h mean) and the PI (24-h mean) were selected within all folds of cross-validation. The combined model outperformed both single-modality models and achieved an AUC = 0.889 (95%-CI: 0.800 to 0.978) and an overall diagnostic accuracy of 87.3%. This is comparable to the 91% accuracy reported when using diffusion-tensor MRI features [34], the 88% accuracy reported using PET features [35], and the 76 to 80% accuracy reported using combined PET/CSF/sMRI features [36, 37]. Our study therefore found evidence that hypoperfusion in individuals can be associated with MCI status, and that ambulatory measurement of BP/CBF can enhance accuracy of MCI detection. Further studies in larger populations are needed to evaluate fully the utility of population-wide ambulatory CBF to diagnose Alzheimer's disease early.

REFERENCES

[1] C. Cordonnier and W. van der Flier, "Brain microbleeds and Alzheimer's disease: innocent observation or key player?," *Brain,* vol. 134 (2), pp. 335-344, 2011.

[2] J. C. de la Torre, "Cerebral hemodynamics and vascular risk factors: setting the stage for Alzheimer's disease," *J. Alzheimer's Dis.,* vol. 32(3), pp. 553-567, 2012.

[3] R. Kelleher and R. Soiza, "Evidence of endothelial dysfunction in the development of Alzheimer's disease: Is Alzheimer's a vascular disorder?," *Am. J. Cardiovasc. Dis.,* vol. 3(4), pp. 197-226, 2013.

[4] A. van Norden, *et al.*, "Dementia: Alzheimer pathology and vascular factors: from mutually exclusive to interaction," *Biochim. Biophys. Acta,* vol. 1822(3), pp. 340-349, 2012.

[5] B. Zlokovic, "Neurovascular pathways to neurodegeneration in Alzheimer's disease and other disorders," *Nat. Rev. Neurosci.,* vol. 12(12), pp. 723-738, 2011.

[6] L. Y. Di Marco, *et al.*, "Vascular dysfunction in the pathogenesis of Alzheimer's disease - A review of endothelium-mediated mechanisms and ensuing vicious circles," *Neurobiol. Disease,* vol. 82, pp. 593-606, 2015.

[7] J. C. de la Torre, "Vascular risk factor detection and control may prevent Alzheimer's disease," *Ageing Res. Rev.,* vol. 9(3), pp. 218-225, 2010.

[8] L. Beishon, *et al.*, "Cerebral hemodynamics in mild cognitive impairment: a systematic review," *J. Alzheimers Dis.,* vol. 59(1), pp. 369-385, 2017.

[9] A. B. Rodell, *et al.*, "Low residual CBF variability in Alzheimer's disease after correction for CO2 effect," *Front. Neuroenergetics,* vol. https://doi.org/10.3389/fnene.2012.00008, 2012.

[10] S. Lattanzi, *et al.*, "Blood pressure variability predicts cognitive decline in Alzheimer's disease patients," *Neurobiol. Aging.,* vol. 35(10), pp. 2282-2287, 2014.

[11] R. Spencer and T. Deak, "A users guide to HPA axis research," *Physiol. Behav.,* p. doi:10.1016/j.physbeh.2016.11.014, 2016.

[12] R. Straub and M. Cutolo, "Glucocorticoids and chronic inflammation," *Rheumatology,* vol. 55(suppl 2), p. ii6, 2016.

[13] P. Boudreau, *et al.*, "A circadian rhythm in heart rate variability contributes to the increased cardiac sympathovagal response to awakening in the morning," *Chronobiol. Int.,* vol. 29(6), pp. 757-768, 2012.

[14] M. Wetherell, *et al.*, "The effects of an anticipated challenge on diurnal cortisol secretion," *Stress,* vol. 18(1), pp. 42-48., 2015.

[15] J. Mattis and A. Sehgal, "Circadian rhythms, sleep, and disorders of aging," *Trends Endocrinol. Metab.,* vol. 27(4), pp. 192-203, 2016.

[16] E. Musiek and D. Holtzman, "Mechanisms linking circadian clocks, sleep, and neurodegeneration," *Science,* vol. 354(6315), pp. 1004-1008, 2016.

[17] H. Chen, *et al.*, " The circadian rhythm of arterial blood pressure in Alzheimer disease (AD) patients without hypertension," *Blood Press.,* vol. 22(2), pp. 101-105, 2013.

[18] M. Nagai, *et al.*, "Hypertension and dementia," *Am. J. Hypertens.,* vol. 23(2), pp. 116-124, 2010.

[19] M. Arbabshirani, *et al.*, "Single subject prediction of brain disorders in neuroimaging: Promises and pitfalls," *NeuroImage,* vol. 145, pp. 137-165, 2017.

[20] G. Orrù, *et al.*, "Using support vector machine to identify imaging biomarkers of neurological and psychiatric disease: a critical review," *Neurosci. Biobehav. Rev.,* vol. 36(4), pp. 1140-1152, 2012.

[21] S. Malm, *et al.*, "Accurate and reproducible measurement of left ventricular volume and ejection fraction by contrast echocardiography: a comparison with magnetic resonance imaging," *J. Am. Coll. Cardiol.,* vol. 44(5), pp. 1030-1035, 2004.

[22] R. Petersen, *et al.*, "Mild cognitive impairment: a concept in evolution," *J. Intern. Med.,* vol. 275(3), pp. 214-228, 2014.

[23] M. Ursino, "Interaction between carotid baroregulation and the pulsating heart: a mathematical model," *Am. J. Physiol. Heart Circ. Physiol.,* vol. 275(5), pp. H1733-H1747, 1998.

[24] R. Lang, *et al.*, "Recommendations for chamber quantification," *Eur. Heart J.-Cardiovasc. Imag.,* vol. 7(2), pp. 79-108, 2006.

[25] B. McDonnell, *et al.*, "Habitual exercise and blood pressure: age dependency and underlying mechanisms," *Am. J. Hypertension,* vol. 26(3), pp. 334-41, 2013.

[26] H. Tanaka, *et al.*, "Aging, habitual exercise, and dynamic arterial compliance," *Circulation,* vol. 102(11), pp. 1270-1275, 2000.

[27] V. van Empel, *et al.*, "Effects of healthy aging on the cardiopulmonary hemodynamic response to exercise," *Am. J. Cardiol.,* vol. 114(1), pp. 131-135, 2014.

[28] G. Mader, *et al.*, "Modeling cerebral blood flow velocity during orthostatic stress," *Ann. Biomed. Eng.,* vol. 43(8), pp. 1748-1758, 2015.

[29] J. Krejza, *et al.*, "Age and sex variability and normal reference values for the VMCA/VICA index," *Am. J. Neuroradiol.,* vol. 26(4), pp. 730-735, 2005.

[30] E. Moradi, *et al.*, "Machine learning framework for early MRI-based Alzheimer's conversion prediction in MCI subjects," *NeuroImage,* vol. 104, pp. 398-412, 2015.

[31] O. C. Okonkwo, *et al.*, "Cerebral blood flow is diminished in asymptomatic middle-aged adults with maternal history of Alzheimer's disease," *Cerebral Cortex,* vol. 24(4), pp. 978-88, 2014.

[32] K. I. Yamashita, *et al.*, "Cerebral blood flow reduction associated with orientation for time in amnesic mild cognitive impairment and Alzheimer disease patients," *J. Neuroimaging,* vol. 24(6), pp. 590-4, 2014.

[33] J. Lin, *et al.*, "Screening for cognitive impairment in older adults: a systematic review for the US Preventive Services Task Force," *Ann. Intern. Med.,* vol. 159(9), pp. 601-612, 2013.

[34] G. Pittam and M. Allaby, "Screening for dementia: Can screening bring benefits to those with unrecognised dementia, their carers and society? An appraisal against UKNSC criteria," UK National Screening Committee, 2014.

[35] S. Haller, *et al.*, "Individual prediction of cognitive decline in mild cognitive impairment using support vector machine-based analysis of diffusion tensor imaging data," *J. Alzheimer's Dis.,* vol. 22(1), pp. 315-327, 2010.

[36] D. Salas-Gonzalez, *et al.*, "Feature selection using factor analysis for Alzheimer's diagnosis using F18-FDG PET images," *Med. Phys.,* vol. 37(11), pp. 6084-6095, 2010.

[37] D. Zhang, *et al.*, "Multimodal classification of Alzheimer's disease and mild cognitive impairment," *Neuromage,* vol. 55(3), pp. 856-867, 2011.

[38] D. Zhang, *et al.*, "Multi-modal multi-task learning for joint prediction of multiple regression and classification variables in Alzheimer's disease," *NeuroImage,* vol. 59(2), pp. 895-907, 2012.